sizes. The histograms of the guinea pigs exposed to antibodies to NGF tended to shift toward larger cell diameters; this shift is more pronounced in the rat (Fig. 1), in that the decrease in cell numbers appears to be due to the loss of cells having diameters less than 30 μm. The shift toward cells of larger diameter in the histograms of both species may indicate either that the largest neurons are less susceptible to antibodies to NGF or that surviving neurons become hypertrophied. It is perhaps more likely that the larger neurons, which develop earlier in gestation (*13*), pass through the phase of NGF dependence before the antibody reaches the fetus [antibody levels in the fetus increase in later stages of gestation (*8*)].

These experiments indicate that most of the sensory neurons in dorsal root ganglia depend for survival on NGF during prenatal development. Our data are quantitatively consistent with experiments showing that most embryonic DRG neurons will survive in vitro in the presence, but not in the absence, of NGF (*3*). The survival of 15 to 20 percent of DRG neurons in the guinea pig may be interpreted as an incomplete destruction of NGF-sensitive neurons, resulting either from an insufficient titer of antibody or access of antibody to their source of NGF, or from a temporal difference in their dependence on NGF. Alternatively, some DRG neurons (up to 20 percent) may not require NGF at any time.

It is not known whether sensory neurons in cranial ganglia are affected by exposure to antibodies to NGF. Deficits observed in the guinea pig (for example, absence of corneal reflex in response to irritants) suggest that at least some of the sensory functions mediated by the trigeminal ganglion are affected. Since sensory neurons in the nodose ganglion are not decreased in number, neurons derived from the placodes, rather than from the neural crest, do not appear to require NGF. This is consistent with the inability of nodose ganglion neurons to retrogradely transport ^{125}I-labeled NGF (*14*). Further studies will be required to resolve the issue of whether cranial sensory ganglia and sensory ganglia that are derived all or in part from the placodes undergo a period of NGF dependence during development.

These data demonstrate that exposure in utero to maternal antibodies to NGF, in addition to producing immunosympathectomy, destroys sensory neurons. Because the developmental anomalies observed in sympathetic and sensory ganglia in familial dysautonomia (*15*) are similar to those observed in the animals described in this report, we suggest that these animals may be a useful model of this human pathological condition. At a more fundamental level, the experimental autoimmune approach should make possible a more precise determination of the time and degree of dependence of different populations of sensory neurons on NGF. The ability to ablate prenatally a significant percentage of the peripheral sensory nervous system will make possible the study of retrograde and anterograde effects of sensory lesions.

EUGENE M. JOHNSON, JR.
PAMELA D. GORIN*
Department of Pharmacology, Washington University Medical School, St. Louis, Missouri 63110
LESLIE D. BRANDEIS
JOHN PEARSON
Department of Pathology, New York University Medical Center, New York 10016

References and Notes

1. R. Levi-Montalcini and P. V. Angeletti, *Physiol. Rev.* **48**, 534 (1968).
2. ———, *Dev. Biol.* **7**, 653 (1963).
3. S. M. Crain and E. R. Peterson, *Brain Res.* **79**, 145 (1974).
4. S. Varon, C. Raiborn, and E. Tyszka, *ibid.* **54**, 51 (1973).
5. S. M. Crain, E. R. Peterson, M. Liebman, H. Schulman, *Exp. Neurol.* **67**, 205 (1980)
6. P. D. Gorin and E. M. Johnson, *Proc. Natl. Acad. Sci. U.S.A.* **76**, 5382 (1979).
7. V. Bocchini and P. U. Angeletti, *ibid.* **64**, 787 (1969). Mouse NGF was kindly supplied by the laboratory of R. Bradshaw.
8. F. W. Brambell, *Frontiers of Biology* (Elsevier, New York, 1970), vol. 18.
9. E. L. Fenton, *Exp. Cell Res.* **59**, 383 (1970).
10. Paraffin sections were cut at 6 μm on a calibrated microtome. In every 20th Nissl-stained section, all neurons containing nucleoli were counted. The total number was obtained by multiplying the summed sample by 20 and correcting for "split" nucleoli by the expression $t/(t + d)$, where t is the thickness of the section and d is the mean nucleolar diameter [E. W. Konigsmark, in *Contemporary Research Methods in Neuroanatomy*, W. H. Nauta and S. O. E. Ebbesson, Eds. (Springer-Verlag, New York, 1970), p. 315]. Multiple nucleoli were accounted for by multiplying the correction by the mean number of nucleoli in a sample of 25 nuclei. Mean nucleolar diameter was corrected for random sectioning by the expression $4\bar{d}/\pi$. [E. R. Weibel, in *Principles and Techniques of Electron Microscopy*, M. A. Hayat, Ed. (Van Nostrand, New York, 1973) p. 237]. Final correction factors ranged from 0.51 to 0.63. Neuron diameters were minimum chords of cells containing nucleoli measured at random when they "passed" a filar micrometer as a mechanical stage was moved in a series of linear sweeps. Pooled samples of 150 measurements from three ganglia were used to construct each distribution histogram.
11. P. D. Gorin and E. M. Johnson, *Dev. Biol.*, in press. The effect on offspring of female rats with comparable antibody titers against mouse NGF shows marked variability as assessed by the size of sympathetic ganglia and tyrosine hydroxylase activity in the ganglia at birth. Possible reasons for this include variability in cross-reactivity of the antibodies to mouse NGF with rat NGF or variability in the time during gestation when antibody is transferred to the fetus. However, in any individual female rat, the severity of effects is consistent from litter to litter. Therefore, the offspring chosen for the analyses reported here were from a female rat that had previously delivered severely affected litters.
12. G. P. Harper *et al.*, *Nature* (*London*) **279**, 160 (1979). The guinea pig NGF used in these experiments was prepared by J. Rubin and R. Bradshaw by a modification of the procedure in (*5*).
13. S. N. Lawson, K. W. T. Caddy, T. J. Biscoe, *Cell Tissue Res.* **153**, 399 (1974).
14. K. Stoeckel, G. Guroff, M. Schwab, H. Thoenen, *Brain Res.* **109**, 271 (1976); E. M. Johnson, R. Y. Andres, R. A. Bradshaw, *ibid.* **150**, 319 (1978).
15. C. M. Riley, R. L. Day, D. M. Greeley, W. S. Langford, *Pediatrics* **3**, 468 (1949); J. Pearson and B. Pytel, *J. Neurol. Sci.* **39**, 47 (1978); ———, N. Grover-Johnson, F. Axelrod, J. Dancis, *ibid.* **35**, 77 (1978).
16. We thank P. Osborne for assistance. This work was supported by the National Foundation–March of Dimes, the Familial Dysautonomia Foundation, and by grants HL20604 and HD12260 from the National Institutes of Health. E.M.J. is an established investigator of the American Heart Association.
§ Present address: Department of Neurobiology, Stanford University, Stanford, Calif. 94305.

4 June 1980; revised 25 July 1980

Fourier-Transformed Infrared Photoacoustic Spectroscopy of Biological Materials

Abstract. *A new technique for measuring the infrared spectra of solids has been developed. The photoacoustic spectra of hemin, hemoglobin, protoporphyrin IX, and horseradish peroxidase show how this technique can be used to obtain structural information about biological materials which cannot readily be studied by normal transmission infrared spectroscopy. The method requires milligram quantities of material and involves no sample preparation.*

It is common in the study of biochemicals that an infrared spectrum of a lyophilized material or an insoluble material is required. Until now, this has been a requirement that could be met only by grinding the material into a KBr wafer or pellet. The possibility of structural alterations resulting from such a procedure is great.

The new technique of Fourier-transformed infrared (FTIR) photoacoustic spectroscopy offers a versatile and convenient solution to this problem. This technique, described briefly below and more fully elsewhere (*1–5*), can be employed for studying the properties of such biological materials. Photoacoustic spectroscopy (PAS) of solid materials in the visible and ultraviolet spectral regions was originally developed in 1881 by Tyndall (*6*), Röntgen (*7*), and Bell (*8*) and has recently been brought back to the forefront of research by Rosencwaig (*9*) and others (*10–13*). However, visible and ul-

0036-8075/80/1121-0918$00.50/0

traviolet PAS spectra often exhibit broad, structureless features. Low and Parodi (*14*) realized that there would be considerable advantages in extending PAS to the infrared region. By using a modified dispersive infrared spectrometer, they were able to measure the infrared-PAS spectra of methanol chemisorbed on silica (*14*). Simultaneously, Busse and Bullemer (*15*) demonstrated that a Fourier-transform infrared spectrometer could be used to obtain infrared PAS spectra of gases in a spectrophone (*15*). By combining these two advances, the technique of FTIR-PAS has been developed.

The method is simple. A small PAS sample cell with a total volume of 1 cm^3 is sealed with an NaCl window to permit the entrance of infrared light from the interferometer head of a Digilab FTS-20 evacuable FTIR spectrometer. The solid sample is placed inside the sample cell. A GR 1962 1/2-inch foil electret microphone (General Radio) picks up the photoacoustic signal generated by the sample when it converts the absorbed infrared light to heat. This microphone output signal is amplified by an Ithaco 143L preamplifier and further processed by the mid-infrared detection electronics of the FTIR spectrometer. The spectrometer Fourier-transforms the resulting photoacoustic interferogram and generates a spectrum of absorbed radiant power against frequency of incident infrared light. The Fourier-transform spectrometer makes these measurements easy because of the multiplexing advantage, the repetitive scanning feature, and the high peak power of the incident infrared light (~ 92 mW for the Digilab FTS-20 spectrometer).

To illustrate the technique with materials of biological interest, we measured the FTIR-PAS spectra of protoporphyrin IX, hemin, hemoglobin, and horseradish peroxidase. They are shown in Figs. 1 through 4. The spectrum of protoporphyrin IX dimethyl ester is qualitatively identical to that reported by Boucher and Katz (*16*). The only quantitative difference is in the relative absorbance of the methyl propionate ester carbonyl stretch at 1738 cm^{-1} seen by the two methods. By comparison with the rest of the spectrum, the PAS signal strength for this band is much less than that reported by Boucher and Katz. This band would be expected to cause high reflectivity by the undiluted sample analyzed by FTIR-PAS at 1738 cm^{-1}, which would not be apparent for a sample pressed into a KBr pellet. This rather important difference demonstrates that FTIR-PAS is sensitive to the reflectivity of the sample; that is, it does not overcome all the difficulties due

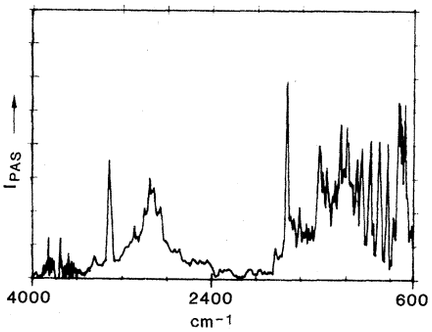

Fig. 1. Spectrum of a 7-mg sample of protoporphyrin IX dimethyl ester (grade 1 purity, Sigma Chemical Co.); 800 scans, resolution 8 cm^{-1}.

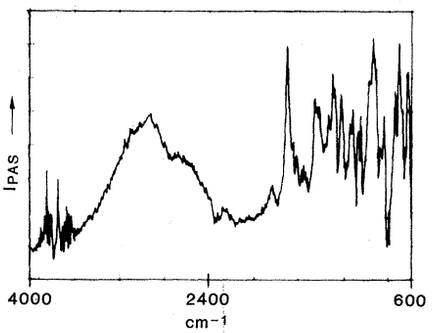

Fig. 2. Spectrum of a 14-mg sample of bovine hemin (grade 1 purity, Sigma Chemical Co.); 800 scans, resolution 8 cm^{-1}.

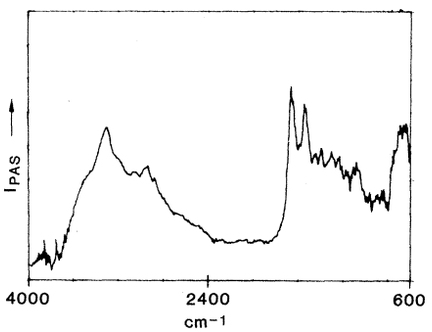

Fig. 3. Spectrum of a 1-mg sample of hemoglobin from beef blood (Sigma Chemical Co.); 800 scans, resolution 8 cm^{-1}.

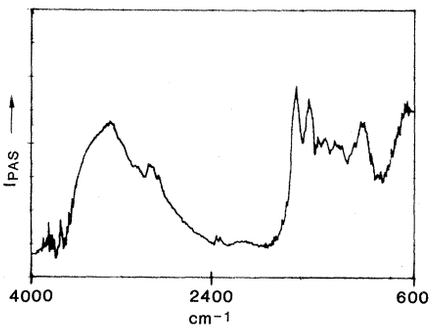

Fig. 4. Spectrum of a 0.5-mg sample of horseradish peroxidase (type VI, Sigma Chemical Co.); 200 scans, resolution 8 cm^{-1}.

to dispersion by the sample which plague attenuated total reflectance techniques. Reflectivity by the sample shows up in the FTIR-PAS spectrum as reduced signal intensity. With this exception, the remarkable agreement between the spectra obtained by the two methods shows that FTIR-PAS is capable of yielding structural information on undiluted solid samples without the need for sample preparation or handling. Experiments are under way to quantitate the dependence of the FTIR-PAS signal on the real and imaginary components of the refractive index of the sample (*17*).

The spectrum of hemin (Fig. 2) is remarkably similar to the conventional transmission spectrum (*18*). It is quantitatively similar except for the diminished intensity of the absorbance at 1708 cm^{-1} in the FTIR-PAS spectrum, which again can be associated with reflection by the sample at this wavelength diminishing the total absorbed power. The sharp absorption due to the N-H stretch in protoporphyrin IX is absent in the spectrum of hemin, as expected. In hemin the nitrogens of the porphyrin ring structure are coordinately bonded to the iron in the center of the ring.

The spectra of hemoglobin and horseradish peroxidase are similar. They show broad, almost structureless absorption, as might be expected. The wealth of different bonds found in the proteins attached to the central porphyrin structure crowd the spectra, with the result that little structural information can be inferred. However, the important fact here is that both of these spectra were measured on samples that were not dissolved in a solvent or pressed into a KBr pellet.

In conclusion, the general applicability of FTIR-PAS to the study of milligram quantities of intact biological samples has been demonstrated. The fact that the samples do not need to be dissolved in a solvent or pressed into a KBr pellet and that the spectra are obtained so conveniently should make this an important addition to the tools available for biochemical analysis. The spectra presented here were obtained at the rate of one scan per second. Thus an 800-scan spectrum was obtained in 13 minutes. However, recent improvements by Digilab in the signal detection section of the FTS-20 spectrometer now make it possible to obtain spectra with a signal-to-noise ratio equivalent to those shown here in one-tenth the time. Although the spectra shown here are presented for the range 4000 to 600 cm^{-1}, the cutoff at 600 cm^{-1} is an arbitrary one dictated by the NaCl window material of the PAS cell. When a cell with cesium iodide windows was

used, PAS spectra were measured to 400 cm^{-1} with this spectrometer. It is much more difficult to measure spectra in the far infrared (< 400 cm^{-1}), however, because of the lack of radiant intensity of the sources used in this region.

M. G. ROCKLEY
D. M. DAVIS
H. H. RICHARDSON
Department of Chemistry,
Oklahoma State University,
Stillwater 74078

References and Notes

1. M. G. Rockley, *Chem. Phys. Lett.* **68**, 455 (1979).
2. _____, *Appl. Spectrosc.* in press.
3. _____ and J. P. Devlin, *ibid.*, in press.
4. M. G. Rockley, *FTS/IR Notes No. 32* (Digilab, Cambridge, Mass., 1980).
5. W. Vidrine, *Appl. Spectrosc.*, in press.
6. J. Tyndall, *Proc. R. Soc. London* **31**, 307 (1881).
7. W. C. Röntgen, *Philos. Mag.* **11**, 308 (1881).
8. A. G. Bell, *ibid.*, p. 510.
9. A. Rosencwaig, *Science* **181**, 657 (1973).
10. _____ and S. S. Hall, *Anal. Chem.* **47**, 548 (1975).
11. W. R. Harshbarger and M. R. Robin, *Acc. Chem. Res.* **6**, 329 (1973).
12. A. Rosencwaig and A. Gersho, *J. Appl. Phys.* **47**, 64 (1976).
13. L. B. Kreuzer, *ibid.* **42**, 2934 (1971).
14. M. J. D. Low and G. A. Parodi, *Appl. Spectrosc.* **34**, 76 (1980).
15. G. Busse and B. Bullemer, *Infrared Phys.* **18**, 255 (1978); *ibid.*, p. 631.
16. L. J. Boucher and J. J. Katz, *J. Am. Chem. Soc.* **89**, 1340 (1967).
17. J. P. Devlin, M. G. Rockley, R. Frech, in preparation.
18. *Sadtler Handbook of Infrared Spectra* (Sadtler Research Laboratories, Inc., Philadelphia, 1967), spectrum 8725k.
19. We gratefully acknowledge support of this work by the National Institutes of Health under grant 5R01GM25353-02 and support by the National Science Foundation for purchase of the FTIR spectrometer (grant CHE78-01764). We thank E. C. Nelson for supplying the samples used in these experiments.

24 April 1980; revised 14 July 1980

Resource Concentration and Herbivory in Oak Forests

Abstract. *Larvae of the fall cankerworm (*Alsophila pometaria*), a polyphagous defoliator of canopy trees, hatch at the time of budbreak of scarlet oak (*Quercus coccinea*), about 10 days before budbreak of white oak (*Quercus alba*). Thus the* Alsophila *population was dense in a site dominated by scarlet oaks and defoliated the scattered white oaks when they came into leaf. In a site dominated by white oaks, the* Alsophila *population was sparse and chiefly attacked scattered scarlet oak. Thus in each stand, the rarer species of tree suffered greater herbivory, in contrast to the more commonly reported observation that herbivore attack on a plant species increases with density.*

The principle that numerically uncommon species may suffer less intense predation than abundant species plays a large role in ecological and evolutionary theory. Predator-prey theory makes frequent recourse to "predator switching," in which predators prey to a disproportionately great degree on the more abundant species of prey (*1*); and in current studies on the interactions between plants and herbivorous insects, the increased herbivory suffered by majority plant species figures largely. Janzen (*2*) and Connell (*3*) proposed that frequency-dependent attack on seeds and seedlings may promote high species diversity in tropical forests; Feeny (*4*) and Futuyma (*5*) suggested that the evolution of chemical diversity among plants may be influenced by the advantages that minority species have in species-rich communities. Several authors (*6*) have documented cases in which herbivory is lower when a plant is grown in polyculture than in monoculture, leading Root (*7*) to postulate that insects will build up where their hosts are most concentrated. We report a counterinstance in which the plant species in the minority suffered greater herbivory.

The study site was about 2 km south of the campus of the State University of New York at Stony Brook, in Suffolk County, where an extensive (≈ 1.3 km^2) woodlot dominated by scarlet oak (*Quercus coccinea*) gives way abruptly (at an ecotone about 300 m wide) to one made up almost exclusively of white oak (*Q. alba*); beyond the ecotone, each of the oaks that is dominant in one area is represented by scattered individuals in the other area. Foliage-feeding lepidopteran larvae are most abundant from late April to early June; of these, larvae of the fall cankerworm *Alsophila pometaria* (Geometridae) are by far the most abundant in most years; they were exceptionally abundant in the spring of 1979. This species hatches at the time of budbreak and completes larval development by the second week of June; as is the case with many other lepidopteran species (*8*), it is incapable of completing development on mature foliage (*9*). The larvae hatch from eggs laid in late fall by wingless females and are dispersed widely by wind, especially in the first instar.

In the course of our studies of *Alsophila* over the last 6 years, we have noted that it consistently hatches at about the time that scarlet oak comes into leaf. White oak does not break bud until about 10 days later. Because *Alsophila* larvae cannot survive for more than 2 to 3 days without food (*9*, *10*), we predicted that the *Alsophila* population should be far more dense in the stand dominated by scarlet oaks than in the white oak stand. Within the white oak stand, *Alsophila* larvae were expected to have a greater impact on the few scarlet oaks than on the white oaks because only scarlet oak is in leaf during the early instars. In the site dominated by scarlet oaks, defoliation of the few white oaks should be heavier than that of scarlet oaks because

Fig. 1. (Left) A white oak in a stand dominated by white oaks, where the population of fall cankerworm is sparse. (Right) A defoliated white oak in a stand dominated by scarlet oaks, where fall cankerworm is abundant. Branches of scarlet oak are visible in the background.

0036-8075/80/1121-0920$00.50/0